3rd Congress of the Alps Adria Acoustics Association
27–28 September 2007, Graz – Austria

NEAR- AND FARFIELD BEAMFORMING USING SPHERICAL LOUDSPEAKER ARRAYS

Franz Zotter[1], Markus Noisternig[2]
[1)] Institute of Electronic Music and Acoustics,
University of Music and Dramatic Arts, 8010 Graz, Austria
(zotter@iem.at)
[2)]LIMSI-CNRS, BP 133, 91403 Orsay Cedex, France
(markus.noisternig@limsi.fr)

Abstract: *Spherical loudspeaker arrays for directivity control in sound wave synthesis are a relatively recent research topic. The accuracy attainable for synthesized directivity patterns mainly depends on three factors: (a) the distance of the target area to the array, (b) the frequency range of interest, and (c) the sound pressure level. In this article, the radiation patterns produced by given array structures, and their frequency-dependent dynamic bounds are studied in-depth. As shown in earlier work, accurate synthesis pattern control is limited towards high frequencies and towards short distances to the array; in both cases this is due to spatial aliasing. The underlying analytical model decomposes the sound field on the surface of the array into spherical harmonics. At a given distance to the array, the attenuation of the spherical harmonic components of the sound pressure depends on the frequency. Therefore, accurate synthesis of directivity patterns requires appropriate near- or farfield equalization. In order to maintain a desired dynamic range of sound pressure level within a given range of distances, it is additionally necessary to introduce a lower frequency limit. This paper discusses these trade-offs analytically, and shows a method how to efficiently implement discrete-time equalization filters.*

Key words: Directivity synthesis, spherical Hankel functions, nearfield sound synthesis

1. INTRODUCTION

Recent studies of directional sound field synthesis with spherical loudspeaker arrays have shown a wide range of applications, including spatial room acoustic measurements, speech communication systems, human computer interaction and sound reinforcement for performing arts. In Caussée [2], and Warusfel [5], [10], both the capture and the re-synthesis of radiation patterns of musical instruments are presented. Kassakian and Wessel [11] studied the limitations and error bounds of directional synthesis for basic array geometries, while recently a practical implementation of a high-order spherical loudspeaker array with programmable radiation patterns was presented by Avizienis [12]. Furthermore, in Behler [9], [13], spatial room acoustic measurements applied to auralisation in architectural acoustics are shown as to be another field of applications.

More comprehensive theoretical frameworks and analytical studies of spherical loudspeakers and arrays are discussed e. g. in Tarnow [1], Meyer [8], and Zotter [14], [15]. Nevertheless, there is a growing demand for further theoretical analysis and verification.

Referring to literature (e. g. Giron [3], Williams [6], Gumerov [7]), the spherical harmonics and the corresponding radial functions (the spherical Hankel and Bessel functions) form a complete set of orthogonal base functions for acoustic radiation problems. According to Warusfel [5], and Meyer [8], these complex-valued radiation patterns, defined on the continuous sphere $\mathcal{S}_n$, are most suitable for radiation pattern synthesis. In real-world systems, a finite number of individually controllable drivers are feasible, e.g. distributed on a sphere $\mathcal{S}_0$ with radius r_0. With these loudspeakers, only a subset of the radiation patterns can be reproduced (with limited bandwidth); the prescribed radiation patterns are either defined by their sound pressure or by their sound particle velocity at a given (primary) synthesis sphere $\mathcal{S}_a$ with given radius $r_a \geq r_0$, cf. Fig. 1.

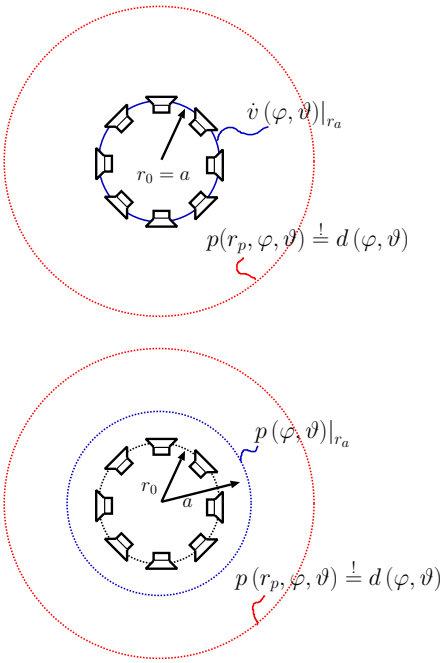

Figure 1: Two basic arrangements for directivity pattern synthesis are shown: In (a) the sound particle velocity distribution $\dot{v}(\varphi,\vartheta)|_{r_a}$ on the sphere with radius $r_a = r_0$ (surface of the array) and in (b) the sound pressure distribution $p(\varphi,\vartheta)|_{r_a}$ on the sphere with radius $r_a > r_0$ are synthesized. In both cases, the synthesis task can be performed in two seperate steps: i) synthesis of spherical harmonic distributions on a primary sphere $\mathcal{S}_a$: *angular beamforming*, ii) projection of these distributions on the target sphere $\mathcal{S}_p$: *radial beamforming*.

To control a desired angular radiation pattern on $\mathcal{S}_a$ (*angular beamforming*) optimal weights for the monophonic loudspeaker signals are derived by its projection onto the array-achievable subspace, cf. Warusfel[10], Behler [9], Kassakian [11]. Once control over a set of spherical harmonics on the *primary sphere* $\mathcal{S}_a$ is obtained, these radiation patterns can be displaced from $\mathcal{S}_a$ onto the *focal sphere* $\mathcal{S}_p$ by applying a set of equalization filters, i.e. *radial beamforming*.

The prescribed radiation patterns are spatially sampled on the sphere by the finite number of drivers, yielding spatial aliasing; i. e. ambiguities between the finite set of spherical harmonics inside and the remaining infinite set outside the controllable bandwidth. Recently a study on the suppression of spherical synthesis errors was presented in [14], also showing criteria to reduce distortions by spatial aliasing. These criteria mainly depend on the aperture radius r_0 of the spherical array and result in a lower bound $r_l \approx 2 \cdot r_0$ for the target radius $r_p \geq r_l$. Moreover, an upper cut-off frequency is given with $f \leq f_u \approx \frac{c}{2 \cdot r_0}$.

The following sections present an in-depth study of the frequency dependent dynamic bounds to accurately synthesize prescribed radiation patterns for given array geometries. First, a brief theoretical review of spherical harmonic functions and analysis is given, cf. [3], [6], and [7]. In particular, spherical Hankel filters for accurate radial near- and farfield beamforming are derived and their dependency on the (primary) synthesis radius r_a and the target radius r_p is shown. A discrete-time implementation of such filters is given and the results are compared with the theoretical results. It is further shown, that the dynamic bounds of the individual drivers introduce limitations on the reproducible bandwidth and target distances[1] of the array.

2. SPHERICAL DIRECTIONAL WAVE FIELD SYNTHESIS

As very common in acoustic theory, the following equations are given in the frequency domain with respect to time. For notational simplicity, the dependency on the frequency variable ω is suppressed. It will be clear from the context of the discussion if the quantity is in the frequency or in the time domain. Therefore, the Fourier transform of the sound pressure $p(\vec{r},\omega)$ and of the sound particle velocity $\vec{v}(\vec{r},\omega)$ become $p(\vec{r})$ and $\vec{v}(\vec{r})$, where $\vec{r}$ represents the position vector.

In the spherical coordinate system with $\vec{r} = (r,\varphi,\vartheta)$ the spherical harmonics represent an eigenspace for the dependency on the angular variables (φ,ϑ), cf. [3][6][7]. Thus the expansion of spherical distributions on $r = const$ into spherical harmonics[2] $Y_n^m(\varphi,\vartheta)$ is convenient. Given the radial sound particle velocity $\dot{v}(\varphi,\vartheta)|_{r_a}$, or the sound pressure $p(\varphi,\vartheta)|_{r_a}$, as a boundary condition on a sphere $\mathcal{S}_a$ with radius r_a (cf. Fig 1), it follows for the spherical wave spectra:

$$\Upsilon_n^m|_{r_a} = \iint_{\mathcal{S}^2} \dot{v}(\varphi,\vartheta)|_{r_a} \cdot Y_n^{m*}(\varphi,\vartheta) \cdot d\Omega, \quad (1)$$

$$\Psi_n^m|_{r_a} = \iint_{\mathcal{S}^2} p(\varphi,\vartheta)|_{r_a} \cdot Y_n^{m*}(\varphi,\vartheta) \cdot d\Omega. \quad (2)$$

where $*$ denotes complex conjugation. With the radial solution of the wave equation, the sound pressure wave resulting from Eq. 1 propagates with:

$$\Psi_n^m(r) = i\rho_0 c \frac{h_n(kr)}{h_n'(kr_a)} \cdot \Upsilon_n^m|_{r_a}, \quad (3)$$

where $k = \omega/c$ is the wave number, $i = \sqrt{-1}$, ρ_0 is the density of air, and c the speed of sound. $h_n(kr)$ is the spherical Hankel function of the second kind[3], and $h_n'(kr)$ its derivative.

Alternatively given Eq. 2, the sound pressure wave yields:

$$\Psi_n^m(r) = \frac{h_n(kr)}{h_n(kr_a)} \cdot \Psi_n^m|_{r_a}. \quad (4)$$

[1] Within this article the expression *target distance* is used in terms of a radial distance to the center of the array, i.e. the origin of the spherical coordinate system. It does *not* denote the distance to the array's surface.

[2] In many textbooks the indices n and m are referred to as *degree* and *order*. However, nomenclature in literature on spatial audio may differ.

[3] The Hankel functions of the second kind are appropriate in causal systems, if the complex exponentials for the Fourier expansion are defined as $e^{i\omega t}$. For $e^{-i\omega t}$ the Hankel functions of the first kind are applicable.

It is worth mentioning, that all sources – representing the *inhomogeneous parts of the soundfield* – have to be situated within the sphere $\mathcal{S}_a$ with radius r_a.

The general signal processing framework of a spherical loudpeaker beamformer is depicted in Fig. 2. It is easy to see, that the radial and angular components of the beamforming algorithm are separated, as will be described in the following sections.

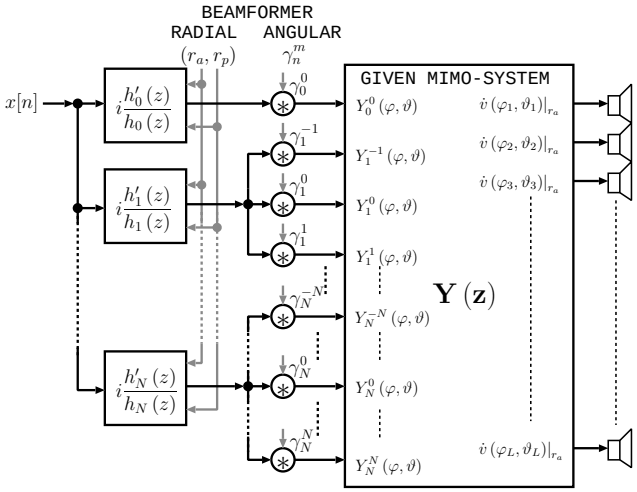

Figure 2: Spherical loudspeaker beamformer.

2.1. Angular Beamformer

Assuming perfect angular pattern resynthesis on the sphere $\mathcal{S}_a$, either the sound particle velocity $\Upsilon_n^m|_{r_a}$ or the sound pressure $\Psi_n^m|_{r_a}$ are given for a finite set of spherical harmonics (n, m) with $n \leq N$ at radius r_a, cf. [14][15]. This may be labeled as *angular beamforming*. The coefficients γ_n^m of a desired angular directivity pattern $\gamma(\varphi, \vartheta)$ are calculated by spherical harmonics analysis as

$$\gamma_n^m = \iint_{\mathcal{S}^2} \gamma(\varphi, \vartheta) \cdot Y_n^{m*}(\varphi, \vartheta) \cdot d\Omega. \quad (5)$$

Therefore, the spherical harmonic coefficients to form a sharp directional lobe $\gamma(\varphi, \vartheta) = \delta(\varphi - \varphi_p, \vartheta - \vartheta_p)$ at direction (φ_p, ϑ_p) may be derived as

$$\gamma_n^m = Y_n^{m*}(\varphi_p, \vartheta_p), \quad (6)$$

where $\delta(\varphi, \vartheta)$ represents the Kronecker delta.

2.2. Radial Beamformer

In order to achieve a desired angular sound pressure distribution at a target (projection) sphere with radius $r = r_p$, a *radial beamformer* is applied. Basically, this radial beamformer is composed of a set of filters $H_n^{(eq)}(\omega)$ to form the inverse of the wave propagation described in Eqs. 3 and 4. It directly follows from the equations that filters for all orders m of the same degree n are equal; the constant multipliers $-1/\rho_0 c$ are omitted to improve readability.

$$H_n^{(eq,v)}(\omega) = i\frac{h_n'(\omega \cdot \Delta t_a)}{h_n(\omega \cdot \Delta t_p)} \quad (7)$$

$$H_n^{(eq,p)}(\omega) = \frac{h_n(\omega \cdot \Delta t_a)}{h_n(\omega \cdot \Delta t_p)} \quad (8)$$

In the equations above, the variables kr_a and kr_p are interpreted as acoustic delays $\Delta t_p = r_p/c$ and $\Delta t_a = r_a/c$ times the angular frequency $\omega = 2\pi f$. This re-formulation proves to be very demonstrative for the interpretation of the simulation results later in this article.

3. DYNAMIC RANGE LIMITS OF THE RADIAL BEAMFORMER

The frequency responses for the radial beamforming filters (Eq. 7) are depicted in Fig. 3. These responses depend on the radius r_0 of the spherical array and the *target* distance r_p for sound field synthesis. An exact calculation of the upper cutoff frequency is given in [14]; above this frequency spatial aliasing occurs. In the following this cutoff frequency is assumed to be $kr_0 \leq \pi$ for simplicity, or $\omega\Delta t_0 \leq \pi$ alternatively.

In this section, we introduce a lower cutoff frequency due to a bounded dynamic range, i.e. *white noise gain* (WNG).

3.1. Example: Simulation of the dynamic playback range, theoretical considerations

In Fig. 3 frequency responses of spherical radial-beamforming filters are presented, derived from a *given sound particle velocity distribution* at radius r_a (cp. Eq. 7). These frequency responses depend on the target distance r_p and on the degree of the spherical harmonics used for synthesis. Assuming a dynamic range for simulations of 40dB WNG, a feasible synthesis bandwidth $ld(\omega_u/\omega_l[n])$ is indicated for different spherical harmonic degrees n; where ω_u refers to the upper and $\omega_l[n]$ to the lower cutoff frequencies respectively. For instance, the IEM's spherical loudspeaker array [15] features an aperture radius of $r_0 = 30cm$, resulting in an upper cutoff frequency of $f_u \approx 600Hz$. The simulation results for a target distance of $r_p = 4 \cdot r_0$ show, that the spherical harmonics of third degree may be reproduced properly with a lower cutoff frequency of $f_l = 150Hz$, whereas the harmonics of second degree are well synthesized above a minimal frequency $f_l = 75Hz$ respectively.

In contrast, the radial beamforming filters shown in Fig. 4 are derived from a given *sound pressure distribution* at distance r_a. The simulation outcomes are comparable to the results based on sound particle velocity distributions, but the curves remain constant over a broad frequency range $\omega\Delta t_a$. In this case, no lower frequency bound for the 40dB WNG dynamic range is indicated.

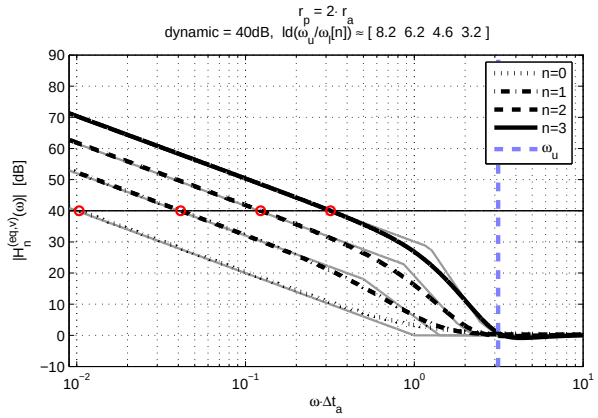

(a) $|H_n^{(eq,v)}(\omega)|$ in dB for $r_p = 2 \cdot r_a$

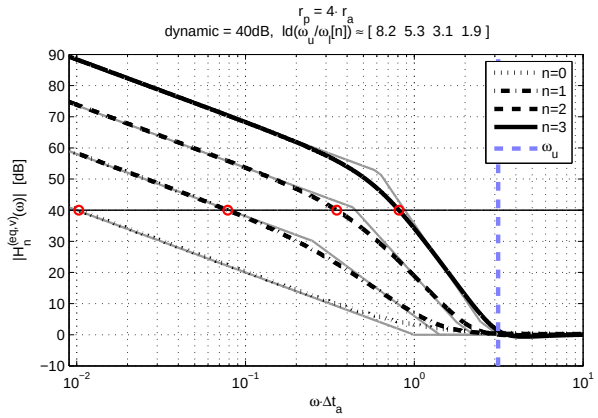

(b) $|H_n^{(eq,v)}(\omega)|$ in dB for $r_p = 4 \cdot r_a$

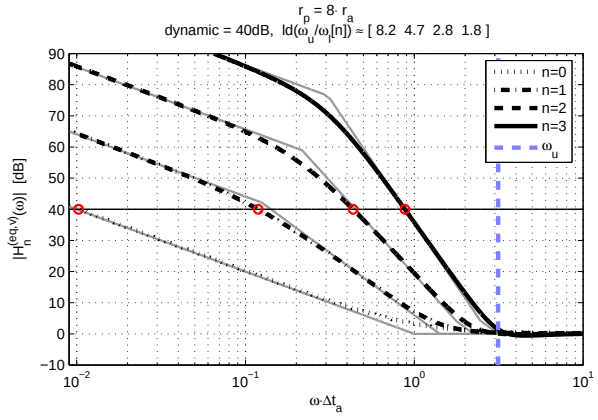

(c) $|H_n^{(eq,v)}(\omega)|$ in dB for $r_p = 8 \cdot r_a$

Figure 3: Frequency responses of spherical radial-beamforming filters subject to different target distances r_p, e.g. (a) $r_p = 2 \cdot r_a$, (b) $r_p = 4 \cdot r_a$, and (c) $r_p = 8 \cdot r_a$, derived from a *given sound particle velocity distribution* at distance r_a, cp. Eq. 7. The feasible bandwidth $ld\,(\omega_u/\omega_l[n])$ for a given dynamic range of 40 dB is indicated. The dashed vertical line indicates the upper cutoff frequency to avoid aliasing, the thin grey lines display the asymptotic approximations of the frequency responses, and the crosspoints illustrate the lower cutoff frequencies.

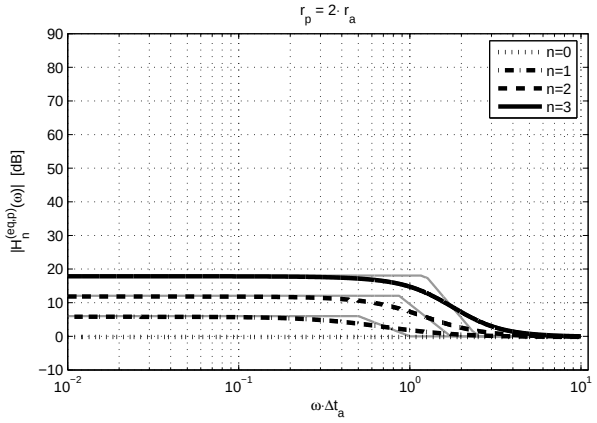

(a) $|H_n^{(eq,p)}(\omega)|$ in dB for $r_p = 2 \cdot r_a$

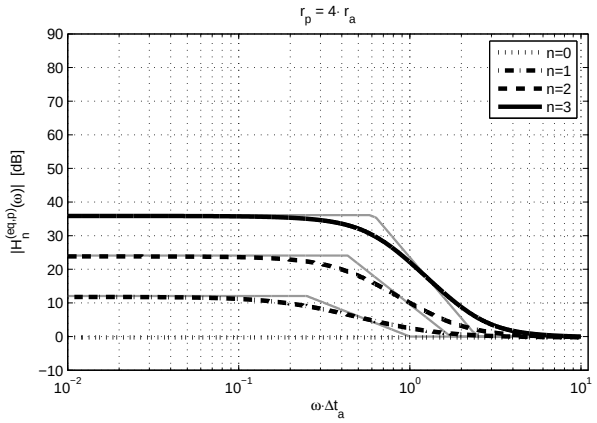

(b) $|H_n^{(eq,p)}(\omega)|$ in dB for $r_p = 4 \cdot r_a$

Figure 4: Frequency responses of radial beamforming filters subject to different target distances r_p, e.g. (a) $r_p = 2 \cdot r_a$ and (b) $r_p = 4 \cdot r_a$ derived from a *given sound pressure distribution* at distance r_a, cp. Eq. 8. The thin gray lines show the asymptotic approximations of the frequency responses.

4. RADIAL BEAMFORMER IMPLEMENTATION

In the following section, discrete-time implementations of radial beamformers for accurate synthesis of directivity patterns are derived. As shown in the analytical model presented above, these spherical equalization filters are defined by ratios of the spherical Hankel functions and their derivatives. Once a discrete-time model of the filters is obtained, it is simply applied to spherical loudspeaker arrays, cf. Fig. 2.

4.1. Spherical Hankel Functions

The spherical Hankel functions of the second kind $h_n(\tilde{\omega})$ and their derivatives $h'_n(\tilde{\omega})$ are defined as follows (cf. [7]):

$$h_n(\tilde{\omega}) = i^{n+1} \frac{e^{-i\tilde{\omega}}}{\rho} \sum_{l=0}^{n} \frac{(n+l)!}{l!\,(n-l)!} \left(\frac{1}{2i\tilde{\omega}}\right)^l \quad (9)$$

$$h'_n(\tilde{\omega}) = -\frac{n-1}{\tilde{\omega}} h_n(\tilde{\omega}) + h_{n-1}(\tilde{\omega}), \quad (10)$$

Note that throughout this article $\tilde{\omega}$ denotes the normalized frequency $\tilde{\omega} = k\,r|_{r=c}$, which simplifies the following

derivations.

4.2. Laplace-Domain

Interpreting Eq. 9 and 10 as a Laplace-Transform of the spherical Hankel functions using $\tilde{s} = i\tilde{\omega}$ yields the following rational functions in $\tilde{s}$:

$$h_n(\tilde{s}) = -i^n \frac{\sum_{k=0}^{n} b_n(k) \cdot \tilde{s}^k}{\tilde{s}^{n+1}} \cdot e^{-\tilde{s}} \quad (11)$$

$$h'_n(\tilde{s}) = i^{n+1} \frac{\sum_{k=0}^{n+1} c_n(k) \cdot \tilde{s}^k}{\tilde{s}^{n+2}} \cdot e^{-\tilde{s}}. \quad (12)$$

The coefficients of the numerator polynomials may be derived using the following difference schemes

$$b_n(n) = 1, \quad \text{for n}\geq 0 \quad (13)$$

$$b_n(k) = \frac{(2n-k-1)(2n-k)}{2\cdot(n-k)} \cdot b_{n-1}(k), \quad \text{for } k < n \quad (14)$$

$$b_n(k) = 0, \quad \text{else}, \quad (15)$$

whereas the coefficients of the derivative of the spherical Hankel functions are given by

$$c_0(k) = -b_1(k), \quad \text{for } 0 \leq k \leq 1 \quad (16)$$

$$c_n(k) = (n+1)\cdot b_n(k) + b_{n-1}(k-2), \quad \text{for } n \geq 1 \text{ and } 0 \leq k \leq n+1. \quad (17)$$

Using the relations above, the polynomials with real-valued coefficients b_r, ω_l, and b_l may be factorized into first- and second-order-sections (FOS, SOS) of the following structure

$$h_n(\tilde{s}) = \frac{1}{\tilde{s}} \cdot \left(\frac{\tilde{s}-b_r}{\tilde{s}}\right)^{mod(n,2)} \times \left(\prod_{l=1}^{div(n,2)} \frac{(\tilde{s}-b_l)^2+\omega_l^2}{\tilde{s}^2}\right), \quad (18)$$

$$h'_n(\tilde{s}) = \frac{1}{\tilde{s}} \cdot \left(\frac{\tilde{s}-b'_r}{\tilde{s}}\right)^{mod(n+1,2)} \times \left(\prod_{l=1}^{div(n+1,2)} \frac{(\tilde{s}-b'_l)^2+\omega'^2_l}{\tilde{s}^2}\right). \quad (19)$$

It is worth mentioning, that for a radial beamformer the different normalizations with Δt_a and Δt_p have to be taken into account when building the ratio of the spherical Hankel functions:

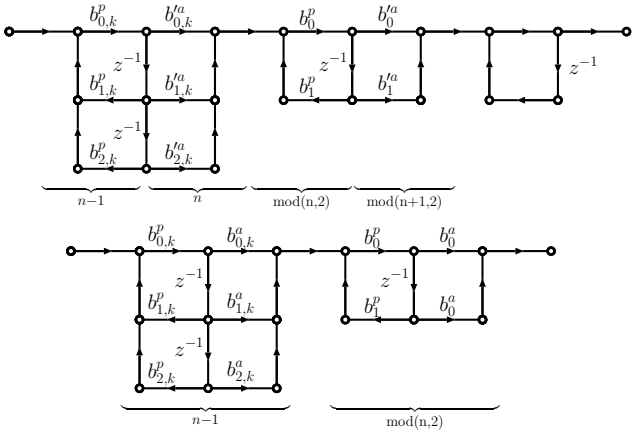

Figure 5: Two examples of digital filter structures for spherical spherical radial-beamforming.

$$h_n(s\Delta t_i) = \frac{1}{s\Delta t_i} \cdot \left(\frac{s-\frac{b_r}{\Delta t_i}}{s}\right)^{mod(n,2)} \times \left(\prod_{l=1}^{div(n,2)} \frac{(s-\frac{b_l}{\Delta t_i})^2+\frac{\omega_l^2}{\Delta t_i^2}}{s^2}\right), \quad (20)$$

$$h'_n(s\Delta t_i) = \frac{1}{s\Delta t_i} \cdot \left(\frac{s-\frac{b'_r}{\Delta t_i}}{s}\right)^{mod(n+1,2)} \times \left(\prod_{l=1}^{div(n+1,2)} \frac{(s-\frac{b'_l}{\Delta t_i})^2+\frac{\omega'^2_l}{\Delta t_i}}{s^2}\right), \quad (21)$$

with $\Delta t_i = \{\Delta t_p, \Delta t_a\}$ depending on the respective radii. In particular, the scaling $\tilde{\omega}\Delta t_a$ and $\tilde{\omega}\Delta t_p$ yields a displacement of the zeros with $b \rightarrow b/\Delta t_i$ and $\omega \rightarrow \omega/\Delta t_i$ by a linear scale factor $1/\Delta t_i$.

4.3. Discrete-Time Implementation of the Radial Beamforming Filters, Impulse Invariance

Applying the impulse invariance technique to the first- and second-order sections[4] in Eq. 20 and Eq. 21, the discrete-time transfer function in z may be derived. The following transform pairs are very useful for calculation:

$$H(s) = \frac{s-b_r}{s} \quad (22)$$

$$\overset{iiv.}{\rightarrow} H(z) = \frac{(1-\tilde{b}_r)-z^{-1}}{1-z^{-1}}, \quad (23)$$

$$H(s) = \frac{(s-b_l)^2+\omega_l^2}{s^2} \quad (24)$$

$$\overset{iiv.}{\rightarrow} H(z) = \frac{1-2\tilde{b}_l+(\tilde{b}_l^2+\tilde{\omega}_l^2+2\tilde{b}_l-2)\cdot z^{-1}+z^{-2}}{(1-z^{-1})^2}. \quad (25)$$

[4] For more accurate results, the interested reader is referred to Cavicchi [4].

The coefficients $\tilde{b}_l$, $\tilde{b}_r$, and $\tilde{\omega}_l$ denote the respective Laplace-domain coefficients scaled by the factor $1/f_s$, where f_s is the sampling frequency. In Fig. 5 an example of the resulting filter structures for radial beamforming is given; Fig. 6 shows the match of the transfer functions to the analytic specifications, assuming parameters suitable for the IEM's icosahedral loudspeaker [15].

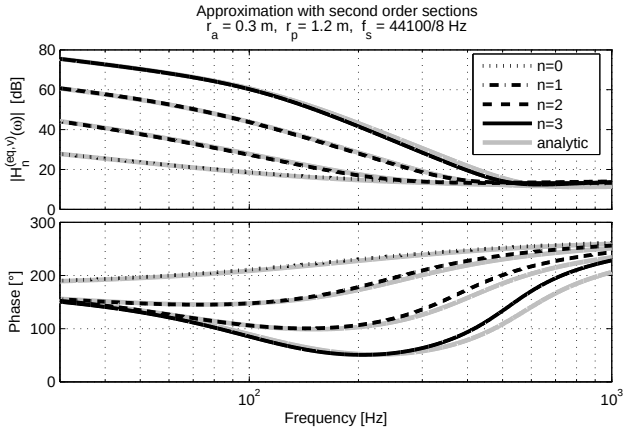

Figure 6: Comparison of frequency responses in magnitude and phase showing the proposed discrete-time radial beamforming filters (black) and their analytic counterparts (gray). A design example using $r_a = 0.3$m, $r_p = 1.2$m, and $f_s = 44100/8$Hz was considered.

5. CONCLUSION

This paper presented a theoretical and simulation analysis of directivity pattern synthesis using spherical loudspeaker arrays. It was shown that accurate sound field synthesis requires appropriate farfield and nearfield equalization. Therefore, equalization filters based on spherical Hankel functions were derived, and ways for efficient discrete-time implementations were discussed. Simulation results were given, revealing a low frequency limit for accurate synthesis, depending on the dynamic range (WNG) of the sound pressure level and a the synthesis target distance. To verify the theoretical results, measurements in an anechoic room will be subject to future research. It is worth mentioning that radial beamforming filters are applicable to a wide range of spherical array applications involving microphones and loudspeakers in open and closed sphere configurations.

6. ACKNOWLEDGEMENTS

We gratefully thank the Zukunftsfonds Steiermark (Prj. 3027) for supporting our research, and most notably Hannes Pomberger for his distinguished work on deriving and testing the implementation of the radial beamforming filters.

REFERENCES

[1] Tarnow, V.: Sound Radiation from Loudspeaker Systems with the Symmetry of the Platonic Solids. Bruel&Kjær, Technical Review 4-1974.

[2] R. Caussé, J.F. Bresciani, and O. Warusfel: Radiation of Musical Instruments and Control of Reproduction with Loudspeakers. ISMA Tokyo, 1992.

[3] Giron, F.: Investigations about the Directivity of Sound Sources. EAA Fenestra, Bochum, 1996.

[4] Cavicchi, T. J.: Impulse Invariance and Multiple-Order Poles. IEEE Tran. Sign. Proc. 44(9), 1996.

[5] O. Warusfel, P. Derogis and R. Caussé: Radiation Synthesis with Digitally Controlled Loudspeakers. 103rd AES-Convention, New York, 1997.

[6] Williams, E. G.: Fourier Acoustics. Academic Press, San Diego, 1999.

[7] N. A. Gumerov and R. Duraiswami: Fast Multipole Methods for the Helmholtz Equation in Three Dimensions. Elsevier, 2004.

[8] P. S. Meyer and J. D. Meyer: Multi Acoustic Prediction Program (MAPP): Recent Results. Presented at the Institute of Acoustics (UK), 2000.

[9] G. Behler: Technique for the Derivation of Wide Band Room Impulse Response. Tecni Acustica, Madrid, 2000.

[10] O. Warusfel and N. Misdariis: Sound Source Radiation Synthesis: from Stage Performance to Domestic Rendering. 116th AES Convention, Berlin, 2004.

[11] P. Kassakian and D. Wessel: Characterization of Spherical Loudspeaker Arrays. 117th AES-Convention, San Francisco, 2004.

[12] R. Avizienis, A. Freed, P. Kassakian, and D. Wessel: A Compact 120 Independent Element Spherical Loudspeaker Array with Programmable Radiation Patterns. 120th AES-Convention, Paris, 2006.

[13] G. Behler: How to Compare Concert Halls by Listening to Music. 4th ASA/ASJ joint meeting, Honolulu, 2006.

[14] F. Zotter, A. Sontacchi, and R. Höldrich: Modeling a Spherical Loudspeaker System as a Multipole Source. 33. DAGA, Stuttgart, 2007.

[15] F. Zotter, and R. Höldrich: Modeling a Radiation Synthesis with Spherical Loudspeaker Arrays. 19th International Congress on Acoustics, Madrid, September, 2007.